5-1-1999

Near-field fluorescence microscopy based on two-photon excitation with metal tips

Erik J. Sánchez

Lukas Novotny

X. Sunney Xie

Citation Details

Sanchez, E. J., Novotny, L. L., & Sunney Xie, X. X. (1999). Near-field fluorescence microscopy based on two-photon excitation with metal tips. Physical Review Letters, 82(20), 4014-4017.

Near-Field Fluorescence Microscopy Based on Two-Photon Excitation with Metal Tips

Erik J. Sánchez,[1,2,*] Lukas Novotny,[1,†] and X. Sunney Xie[1,2,*]

[1]*William R. Wiley Environmental Molecular Sciences Laboratory, Pacific Northwest National Laboratory, P.O. Box 999, Richland, Washington 99352*

[2]*Department of Physics/Environmental Science and Resources Program, Portland State University, P.O. Box 751, Portland, Oregon 97207-0751*

(Received 6 January 1999)

We present a new scheme for near-field fluorescence imaging using a metal tip illuminated with femtosecond laser pulses of proper polarization. The strongly enhanced electric field at the metal tip ($\approx$15 nm end diameter) results in a localized excitation source for molecular fluorescence. Excitation of the sample via two-photon absorption provides good image contrast due to the quadratic intensity dependence. The spatial resolution is shown to be better than that of the conventional aperture technique. We used the technique to image fragments of photosynthetic membranes, as well as *J*-aggregates with spatial resolutions on the order of 20 nm. [S0031-9007(99)09142-5]

PACS numbers: 07.79.Fc, 42.50.Hz, 87.64.Vv, 87.64.Xx

The general aim of near-field optics is to extend optical microscopy beyond the diffraction limit. The introduction of the aperture probe for near-field microscopy [1,2] has allowed fluorescence imaging below the diffraction limit and has stimulated interests in many disciplines, especially the material and biological sciences. The widely adapted aperture approach is based on an aluminum-coated fiber tip [2] of which the foremost end is left uncoated to form a small aperture. Unfortunately, only a tiny fraction ($<10^{-4}$ for a 100 nm aperture) of the light coupled into the fiber is emitted by the aperture because of the cutoff of propagation of the waveguide modes. The low light throughput and the finite skin depth of the metal are the limiting factors for resolution. Many applications require spatial resolutions that are not obtainable with the aperture technique. For example, in the effort on spectroscopic imaging of photosynthetic membranes [3], a spatial resolution of at least 20 nm was desired in order to resolve closely packed individual proteins in a lipid membrane. Moreover, the aperture technique has other practical complications: (1) It is difficult to obtain a smooth aluminum coating on the nanometric scale which introduces nonreproducibility in probe fabrication, as well as measurements; (2) the flat ends of the aperture probes are not suitable for simultaneous topographic imaging of high resolution; (3) the absorption of light in the metal coating causes significant heating and poses a problem for biological applications. To overcome these limitations, we present a new approach for high-resolution fluorescence imaging based on a sharp, laser-illuminated metal tip.

The use of laser-illuminated metal tips for near-field imaging has been discussed by many groups [4–13]. Most of the work has been limited to light scattering at the metal tip. The tip locally perturbs the fields at the sample surface; the response to this perturbation is detected in the far field at the same frequency of the incident light. The detected signals contain both near-field and far-field contributions and are generally dominated by topographic rather than spectroscopic information. The interpretation of the contrast in the recorded images is difficult.

In this Letter, we use the metal tip to provide a local excitation source for the spectroscopic response of the sample under investigation. The underlying principle of this approach has been outlined in a previous paper [11]. Excitation light of proper polarization induces a strongly enhanced field at the tip. The enhanced field consists mainly of nonpropagating (evanescent) components and is, thus, strongly confined to the tip end. The enhanced fields locally interact with the sample surface and generate a spectroscopic response that is detected in the far field at a different wavelength. The enhanced field at a gold tip is used here as a two-photon excitation source for molecular fluorescence. However, the same concept can be applied to other forms of linear and nonlinear imaging, such as imaging based on surface enhanced Raman scattering.

Rigorous electromagnetic calculations for a laser-illuminated ($\lambda = 800$ nm) gold tip with an end diameter of 10 nm have shown an intensity enhancement factor of roughly 3000 over the incident light [12]. We note that the incident wavelength is far away from the surface plasmon resonance. The field enhancement arises from a high surface charge density at the tip that is induced by the incident light polarized along the tip axis. In contrast, incident light with polarization perpendicular to the tip axis results in no field enhancement [11–13]. For a symmetrical tip perpendicular to a sample surface, the desired polarization for the field enhancement can be provided by side-on illumination. However, this leads to a large illumination area, giving rise to an overwhelming background signal. It was proposed that a tightly focused higher-order laser mode with a strong longitudinal field could be used for on-axis illumination [11]. In this work, we take the simpler approach of fabricating an asymmetrical metal tip. Figure 1(a) shows a field emission electron micrograph of a gold tip with an end diameter of 15 nm fabricated with etching and

 0031-9007/99/82(20)/4014(4)$15.00

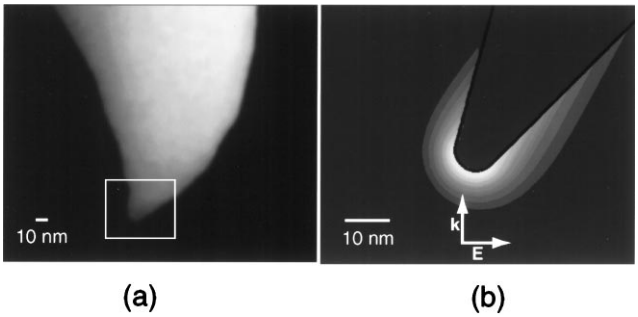

FIG. 1. (a) Scanning electron micrograph of an asymmetrical gold tip fabricated by FIB in order to achieve field enhancement with the horizontal polarization of a focused laser beam. (b) Calculated intensity distribution near a gold tip mimicking the tip in (a); k and E indicate the propagation direction and the polarization of the incident field, respectively. An enhancement factor of 1000 in intensity over the incident light is present at the tip end.

subsequent focused ion beam (FIB) milling [14–16]. Because of the bent shape, the field enhancement can be excited by light polarized in the horizontal direction, as is the case for a TEM_{00} focused laser beam along the upward direction. Figure 1(b) shows the calculated field intensity distribution at the end of a symmetrical gold tip tilted from the vertical direction mimicking the situation in Fig. 1(a). The electric field intensity at the tip end is found to be enhanced by a factor of $f \approx 1000$. The calculated fields are rigorous three-dimensional solutions of Maxwell's equations obtained by the multiple multipole approach (as in [11,12]). Calculations for a 10-nm gold sphere showed that the enhancement factor is 2 orders of magnitude lower compared to the gold tip. Although a higher enhancement factor can be expected for silver, we found that this material generates a white-light continuum background signal stronger than gold when irradiated by femtosecond pulses of moderate power.

A key issue in near-field fluorescence imaging with metal tips is the rejection of the background signal from the entire illuminated area. In order to enhance the near-field contrast, we utilized two-photon excitation of fluorescence [17]. Since two-photon excitation is a nonlinear process with quadratic dependence on excitation intensity, the detected fluorescence signal becomes proportional to the square of the intensity enhancement factor $f^2 \approx 10^6$. Assuming that the illuminated area of a uniform two-dimensional fluorescent sample is S (10^5 nm^2 for a tightly focused beam) and the intensity enhanced area underneath the tip is σ (100 nm^2), the signal-to-background ratio for one-photon excitation is expected to be $f\sigma/S = 1$. In contrast, for two-photon excitation, the signal-to-background ratio is $f^2\sigma/S = 1000$. Therefore, two-photon excitation leads to a significantly improved contrast.

The schematic of our apparatus is shown in Fig. 2. The light source for two-photon excitation is a mode-locked Ti-sapphire laser (Coherent Mira 900) providing 100 fs pulses of 830 nm at a repetition rate of 76 MHz. The beam is sent into an inverted fluorescence microscope (Nikon TE300), reflected by a dichroic beam splitter (Chroma Mdl. 725DCSP) and focused by a microscope objective (Nikon apochromatic, 60×, 1.4 NA) on the sample surface. The metal tip, held above the sample surface in close proximity, is centered onto the focal spot. The average excitation power was attenuated to 5–30 μW at the diffraction-limited focal spot. At this power level, heating of the tip is negligible [12]. Fluorescence was collected by the same objective lens, filtered by the combination of the dichroic filter and three interference filters, and detected by either a photon-counting avalanche photodiode (EG&G SPCM 200) or a combination of a spectrograph (Acton 150) and an intensified charged couple device (Princeton Instruments, Pentamax). The sample was mounted on a 50 × 50 μm^2 closed-loop scan bed (Physik Instrumente) and raster scanned in the horizontal plane. Most images are composed by 256 × 256 pixels with a line scan rate of 0.2 to 0.4 Hz. The entire microscope is placed inside a light-free, acoustically damped enclosure located on a floating optical table.

The metal tip is maintained within 2 nm above the sample surface by using a tuning-fork feedback mechanism [18]. A highly sensitive preamplification allows operation with the interaction forces between tip and sample being 10 to 100 pN. Because forces in this range do not affect the soft gold tips, the tips maintained their sharpness after scanning many images. We implemented a phase-sensitive detection scheme [19,20] with a fast time response to circumvent the limitations imposed by the high Q factor (≈1600) of the tuning-fork resonance. The vertical noise (electrical and mechanical) of the entire system is less than 0.2 nm.

The use of a metal tip only a few nanometers away from a chromophore raised concerns about fluorescence quenching by the metal tip. Fortunately, this problem was minimized for samples of molecular aggregates such as J-aggregates and fluorescent proteins in photosynthetic membranes. In particular, pseudoisocyanine (PIC) dye

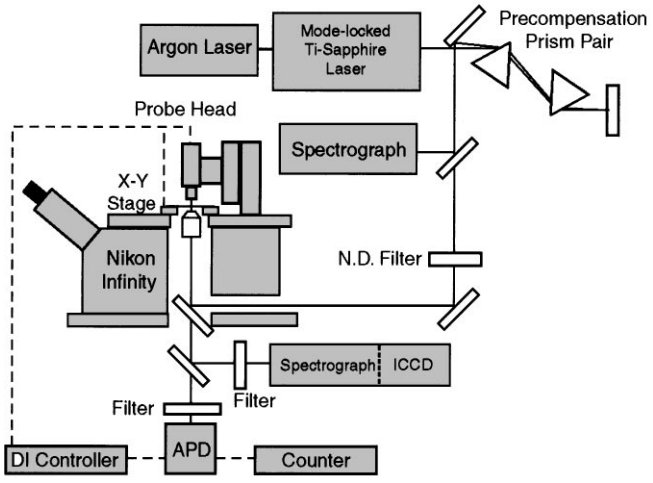

FIG. 2. Experimental apparatus. See text for details.

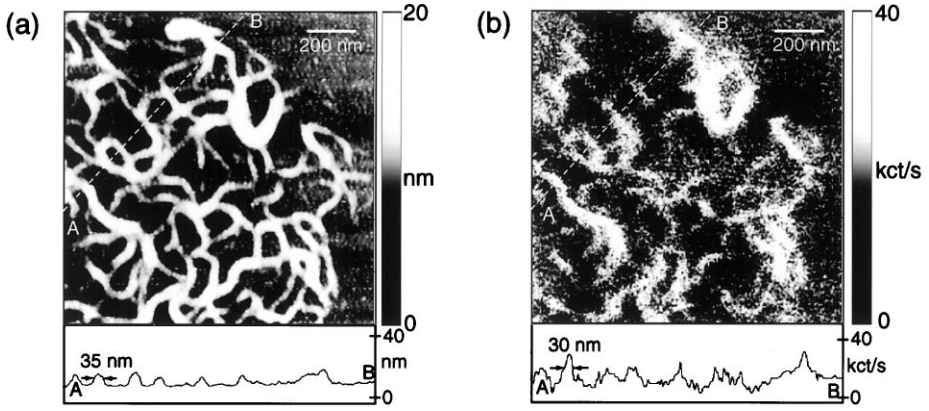

FIG. 3. Simultaneous topographic image (a) and near-field two-photon excited fluorescence image (b) of *J*-aggregates of PIC dye in a PVS film on a glass substrate. The topographic cross section along the dashed line (A-B) has a particular feature of 35-nm FWHM (indicated by arrows) and a corresponding 30-nm FWHM in the emission cross section.

molecules of *J*-aggregates have extremely fast energy transfer along the aggregate length with an upper bound of coherent length of 50 nm [21], whereas the chlorophyll a (Chl a) and chlorophyll b (Chl b) molecules in light harvesting complex (LHCII) are separated by only a couple of nanometers according to the crystal structure [22]. Rapid energy transfer in these systems allows the fluorescence emission to take place far from the metal tip so that fluorescence quenching by the metal is reduced.

Figures 3(a) and 3(b) show the simultaneous images of topography and near-field two-photon excited fluorescence for *J*-aggregates of PIC dye molecules in polyvinyl sulfate (PVS). The method of sample preparation has been described by Higgins *et al.* [21]. The lower portions of Fig. 3 show the simultaneous cross sections taken across the aggregate strands (dotted white line). The arrows in the topography cross section indicate a feature with FWHM of 35 nm, while the corresponding feature in the emission cross section has a FWHM of 30 nm. This image demonstrates the superior spatial resolution of the present approach.

To further prove the near-field contrast, Fig. 4(a) shows the tip approach curve for the emission signal as a function of tip-sample distance at a particular point of an aggregate strand. The rapid decay of the emission signal at a tip-sample distance comparable to the tip diameter provides a clear proof of the principle of our approach.

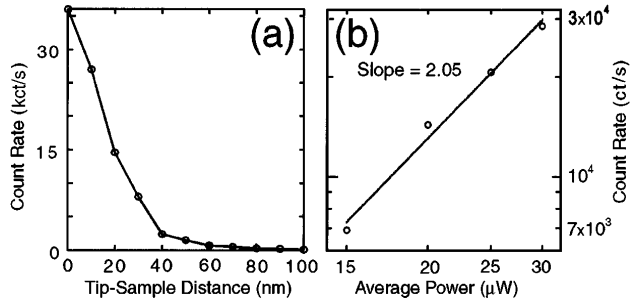

FIG. 4. (a) Emission signal as a function of the tip-sample distance at a particular spot of a PIC *J*-aggregate strand. (b) Log-log plot of the emission signal as a function of the average power of the incident light with the tip on top of an aggregate strand.

Figure 4(b) shows the dependence of the emission signal on the average incident power while the tip was on top of an aggregate strand. The quadratic dependence proves the two-photon excited emission.

The emission spectrum of the brightest feature near the upper center of the image is shown in Fig. 5(a). With an excitation power level of $\approx 15\ \mu$W and an acquisition time of 1 sec, the dotted line indicates the far-field contribution with no gold tip present. The solid line with a peak at 575 nm corresponds to the emission from *J*-aggregates with the gold tip present, which is similar to the far-field spectrum of the same sample. Although white-light continuum generation with gold tips was observed at higher power levels, no indication of such an emission occurred at the power levels at which the images were taken.

Figure 5(b) shows the near-field emission spectrum of a sample of photosynthetic membrane fragments from the *chlamydomonas reinhardti* strain (C2 mutant, doubly deficient in photosystem I and photosystem II [3]). The dotted line is the emission spectrum recorded when the tip was lifted. Figures 6(a) and 6(b) show the simultaneous images of topography and fluorescence of the sample, respectively. The topographic image indicates that micelles were formed when the membrane fragments were placed on the glass slip and allowed to dry. LHCII proteins embedded in lipid membrane have naturally fluorescent Chl a and Chl b molecules that are subject to two-photon excitation to the Soret band. The excitation

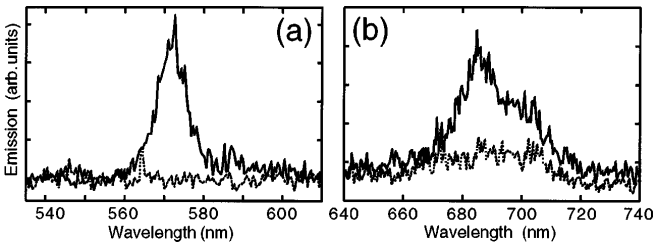

FIG. 5. (a) Fluorescence emission spectrum of PIC *J*-aggregates obtained with (solid line) and without (dotted line) the tip present. (b) Fluorescence emission spectrum of Chl a and Chl b from LHCII proteins obtained with (solid line) and without (dotted line) the tip present.

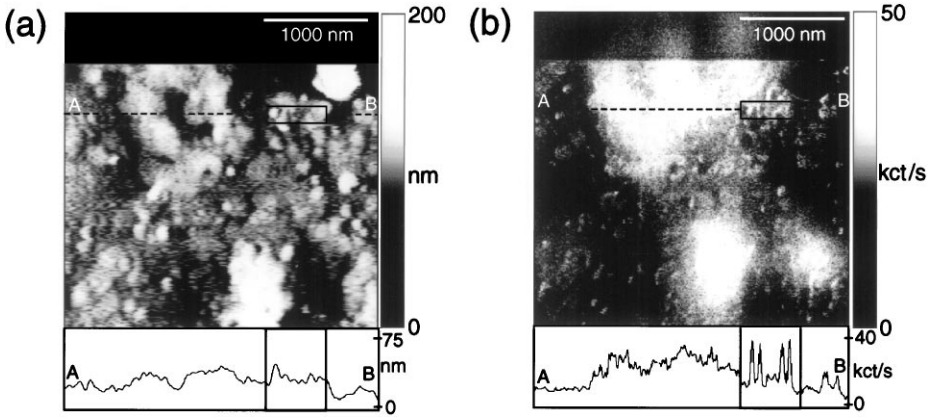

FIG. 6. Simultaneous topographic image (a) and near-field two-photon excited fluorescence image (b) of photosynthetic membrane fragments from *chlamydomonas reinhardti* (C2 mutant) algae on a glass substrate. The corresponding topographic and emission cross sections along the dashed lines (A-B) are shown. The four emission peaks in the box have a FWHM of ≈20 nm.

light at 830 nm had an average power level of ≈25 μW. The dark region on the top is the region with the tip not present, resulting from only the far-field contribution with diffraction-limited resolution. When the tip was lowered to the surface, the near-field contrast appeared with many fluorescent features. The simultaneous images allowed correlation of the topographic and spectroscopic information. The high topographic feature (≈400 nm) in the upper right-hand corner did not give any fluorescence signal. Most of the fluorescence features are correlated with topographic features. The cross sections below in Fig. 5(b) show four fluorescent features which all have a FWHM of ≈20–30 nm and similar intensities. Some features in the fluorescence image are on the order of 15 nm, with a signal-to-background ratio of better than 10:1. Transmission electron microscope micrographs as well as electron crystallography have shown that the trimer LHCII protein has a two-dimensional unit cell dimension of ≈13 nm [22,23], containing at least 7 Chl a and 5 Chl b per monomer [22]. We tentatively attribute the four peaks to individual units of LHCII in the micelles. The same features show up in the retrace images but reduced in emission intensity due to photobleaching. The spatial resolution of our method is approaching the limit of the size of individual protein molecules inside biological membranes.

We thank Khaled Karraï for advice on the tuning-fork feedback mechanism, Jim Follansbee and David Prior for assistance with electronic circuit design, Jim Young for use of the electron microscope facilities, Peter Reike and Mark Englehard for use of the FIB components, and Lauren Mets for algae samples. This research was supported by the U.S. Department of Energy's (DOE) Office of Basic Energy Sciences, Chemical Sciences Division. Pacific Northwest National Laboratory is operated for DOE by Battelle under Contract No. DE-AC06-76RLO 1830.

*Present address: Department of Chemistry and Chemical Biology, Harvard University, 12 Oxford Street, Cambridge, Massachusetts 02138.

†Present address: The Institute of Optics, University of Rochester, Rochester, New York 14627.

[1] D. W. Pohl, W. Denk, and M. Lanz, Appl. Phys. Lett. **44**, 651 (1984); A. Lewis, M. Isaacson, A. Harootunian, and A. Murry, Ultramicroscopy **13**, 227 (1984).
[2] E. Betzig *et al.*, Science **251**, 1468 (1991); E. Betzig and J. K. Trautman, Science **257**, 189 (1992).
[3] R. C. Dunn, G. R. Holtom, L. Mets, and X. S. Xie, J. Phys. Chem. **98**, 3094 (1994).
[4] S. Kawata and Y. Inouye, Ultramicroscopy **57**, 313 (1995).
[5] F. Zenhausern, M. P. O'Boyle, and H. K. Wickramasinghe, Appl. Phys. Lett. **65**, 1623 (1994).
[6] P. Gleyzez, A. C. Boccara, and R. Bachelot, Ultramicroscopy **57**, 318 (1995).
[7] J. Jersch and K. Dickman, Appl. Phys. Lett. **68**, 868 (1996).
[8] W. Denk and D. W. Pohl, J. Vac. Sci. Technol. **9**, 510 (1991).
[9] A. A. Gorbunov and W. Pompe, Phys. Status Solidi A **145**, 333 (1994).
[10] A. V. Bragas, S. M. Landi, and O. E. Martínez, Appl. Phys. Lett. **72**, 2075 (1998).
[11] L. Novotny, E. J. Sánchez, and X. S. Xie, Ultramicroscopy **71**, 21 (1998).
[12] L. Novotny, R. X. Bian, and X. S. Xie, Phys. Rev. Lett. **79**, 645 (1997).
[13] O. J. F. Martin and C. Girard, Appl. Phys. Lett. **70**, 705 (1997).
[14] M. J. Vasile *et al.*, Rev. Sci. Instrum. **62**, 2167 (1991).
[15] J. Orloff, Rev. Sci. Instrum. **64**, 1105 (1993).
[16] E. J. Sánchez, Ph.D. thesis, Portland State University, Portland, OR, 1999.
[17] W. Denk, J. H. Strickler, and W. W. Webb, Science **248**, 73 (1990).
[18] K. Karrai and R. D. Grober, Appl. Phys. Lett. **66**, 1842 (1995).
[19] A. G. T. Ruiter *et al.*, Ultramicroscopy **71**, 149 (1998).
[20] T. R. Albrecht, P. Grutter, D. Horne, and D. Rugar, J. Appl. Phys. **69**, 669 (1991).
[21] D. A. Higgins and P. F. Barbara, J. Phys. Chem. **99**, 3 (1995).
[22] W. Kühlbrandt, D. N. Wang, and Yoshinori Fujiyoshi, Nature (London) **367**, 614 (1994).
[23] For a review, see K. R. Miller, *Electron Microscopy in Biology*, edited by J. D. Griffith (John Wiley & Sons, New York, 1995), pp. 1–30.